Isothermal crystallization of nylon 6/liquid crystal copolyester blends[☆]

I. Campoy, M.A. Gómez*, C. Marco

Instituto de Ciencia y Tecnología de Polímeros (CSIC), Juan de la Cierva 3, 28006 Madrid, Spain

Abstract

The isothermal crystallization behaviour has been investigated for several compositions of blends between nylon 6 (N6) and the liquid crystal copolyester Vectra using calorimetric and X-ray diffraction techniques. Differences in the crystallization rates have been related to the structural properties of these systems by means of WAXS and SAXS real time experiments using synchrotron radiation. Other kinetic parameters such as the Avrami exponents, the equilibrium melting temperatures, and the interfacial free energies have been determined from the calorimetric data. © 1999 Elsevier Science Ltd. All rights reserved.

1. Introduction

It is well known that the physical and mechanical properties of crystalline polymers depend on the morphology, the crystalline structure, and the degree of crystallization. Thus, considerable attention have been paid to the crystallization processes in high polymers suitable for extrusion and/or moulding purposes [1].

This analysis is far more complex in the case of binary blends [2] and most of the information reported in the literature is concerned with completely miscible blends, but the crystallization kinetics of partially miscible or immiscible blends has not been extensively studied. The most important factors affecting the crystallization of these systems correspond to the effect of blend composition, processing and crystallization conditions on the morphology, the primary nucleation, the rate of crystallization, the crystallinity, and other structural parameters such as long spacing. Only a few studies have been published about the crystallization kinetics of blends between a liquid crystal copolyester and a thermoplastic polymer [3,4]. Most of the available information is only related to mechanical and rheological properties, although parameters such as the crystallization rate can strongly influence the solidification processes and the production costs.

The crystallization kinetics of nylon 6 (N6) was investigated widely [5–13] caused by its technological interest in manufacturing processes. The crystallization rates or the mechanism of crystallization and growth have been studied as the mechanical properties of polyamides, such as tensile or frictional properties, are controlled by the degree of crystallization or the morphology of the supramolecular structures [14,15].

Another point of interest is related to the thermodynamic and kinetic parameters of crystallization that determine the formation of different crystalline forms and their phase transitions. The thermal and structural properties of blends between N6 and the commercial thermotropic copolyester Vectra A have been reported in a previous paper [16] and the effect of the thermal history and the liquid crystal content in the formation of different polymorphic modifications of N6 has been determined. In this paper, we have investigated the isothermal crystallization of these blends by means of differential scanning calorimetry (DSC), small angle X-ray diffraction (SAXS) and wide angle X-ray diffraction (WAXS), in order to clarify the mechanism of the polymorphic transitions in N6 and the effect of the addition of the liquid crystal component. The use of synchrotron radiation for the X-ray experiments has been very useful for this purpose as it has been possible to follow in real time the structural changes of these materials during the crystallization process.

2. Experimental

The thermotropic liquid crystal copolyester used in this

[☆] Dedicated to the memory of Prof. Fatou.
* Corresponding author. Tel.: +34-915622900-x-310; Fax: +34-915644853.
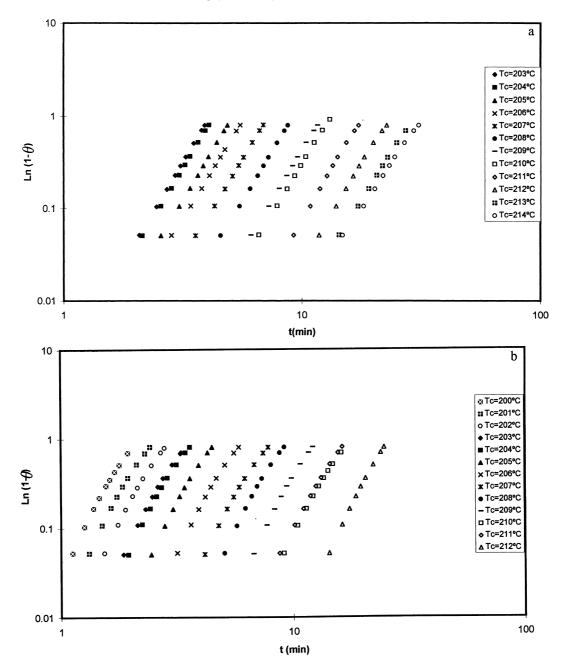*E-mail address:* ictgr01@pinarl.csic.es.

Fig. 1. Double logarithmic plot of $1 - \theta(t)$ against time for (a) 100/0 and (b) 90/10 N6/Vectra A blends at the indicated temperatures.

study is the commercial product Vectra A 950 from Hoechst Iberica SA, a wholly aromatic copolyester consisting of 27 mol% 2-6 hydroxynaphthoic acid (HNA) and 73 mol% p-hydroxybenzoic acid (HBA). Nylon 6 Akulon K123 was supplied by La Seda S.A.

Both polymer pellets were dried in an oven at 120°C for 24 h. Blending was done in a Haake Rheocord System 60 rheometer equipped with a 60 gr mixing head. The temperature was set at 290°C and the rotor speed at 50 rpm. Mixing was done for 5 min until the torque became stabilized and samples were slowly cooled down to room temperature. Eleven compositions of blends N6/Vectra were prepared

in the ratios of 100/0, 99/1, 98/2, 95/5, 90/10, 85/15, 70/30, 50/50, 30/70, 15/85 and 0/100 by weight. The blends obtained directly from the Haake Rhecord System 60 were prepared as powder samples by grounding.

Differential scanning calorimetry (DSC) measurements were performed under isothermal conditions using a Perkin-Elmer DSC 7/7700 calorimeter. Automatic calibration was carried out using indium ($T_m = 156.5$°C, $\Delta H_m = 28.45$ J g^{-1}) and zinc ($T_m = 419.47$°C, $\Delta H_m = 108.37$ J g^{-1}) as standards.

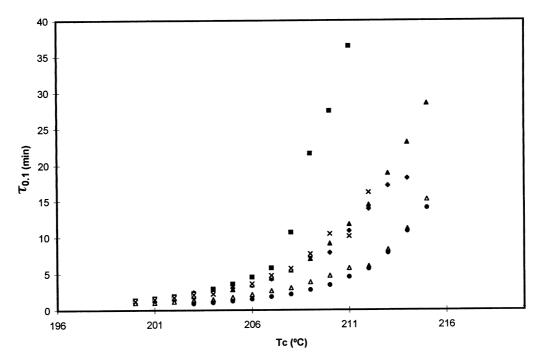The kinetic studies were done by calorimetric techniques using the principles described by Fatou and Barrales

Fig. 2. Plot of $\tau_{0.1}$ against crystallization temperature for the following N6/Vectra blend compositions: (◆) 100/0, (■) 99/1, (▲) 98/2, (×) 90/10, (△) 85/15, (●) 70/30.

elsewhere [17]. The samples were heated to 240°C and the temperature was kept for 5 min. Subsequently, the samples were cooled at a rate of 64°C min^{-1} to the desired temperature and the corresponding exotherms were scanned as a function of time until no change was observed in the DSC baseline. Partial areas, corresponding to a given percentage of the total transformation, were determined from the data points stored, for each isothermal run on a PE 7700 computer, using DSC7 kinetic software. After completion of crystallization, the transition temperatures were detemined by heating the samples at a rate of 10°C min^{-1}.

The crystallinity degree of the N6 phase, $(1 - \lambda)$, was determined by calorimetric analysis using the following relation:

$$1 - \lambda = \frac{\Delta H_{N6}}{\Delta H_{N6\,100\%}\,*w_{N6}}$$

where ΔH_{N6} is the apparent enthalpy of melting of N6, w_{N6} is the weight fraction of N6 in the blends and $\Delta H_{N6\,100\%}$ is the extrapolated value of the enthalpy corresponding to the melting of 100% crystalline sample. A mixture of α and γ^* crystalline forms of N6 is observed in most of the samples analyzed in this paper and for this reason, an average value of 190 J g^{-1} have been chosen for $\Delta H_{N6\,100\%}$. As it was described in a previous paper [16], several values were proposed for the enthalpy of melting for the different 100% crystalline polymorphic forms of N6. An intermediate value of 190 J g^{-1} was reported by Ioune [18], using several N6 samples with different molecular weights and crystallinities and plotting the heat of fusion obtained by calorimetric

techniques from the area under the peak against the crystallinity determined by density measurements.

Wide and small angle X-ray diffraction patterns were recorded simultaneously using synchrotron radiation at the polymer beam line at Hasylab (DESY, Hamburg). The beam was monochromatized (1.5 Å) by Bragg reflection through a germanium single crystal in order to focus the beam in a horizontal direction. For focussing in the vertical direction a mirror was used. The scattering was detected with a linear Gabriel detector. Further details concerning the instrument are given elsewhere [19]. The scattering intensity was divided by the intensity of the primary beam, as measured by an ionization chamber in relative units, in order to consider the change of the intensity of the primary beam during the measurements. The background scattering obtained when no samples were present in the beam was subtracted from all measured curves after proper correction with respect to absorption. The design of the crystallization kinetics experiments were similar to those described above for the calorimetric experiments.

3. Results and discussion

The crystallization kinetics of the N6 pure homopolymer and in blends up to 30% of Vectra A were systematically investigated by DSC, WAXS and SAXS under isothermal conditions. To the best of our knowledge, no such studies for blends of this type have been published. A thermogravimetric study of these systems has been previously done in
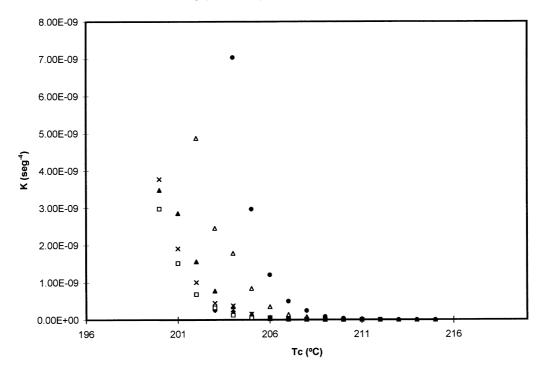
Fig. 3. Plot of *K* values against crystallization temperature for the following N6/Vectra blend compositions: (◆) 100/0, (□) 99/1, (▲) 98/2, (×) 90/10, (△) 85/ 15 (●) 70/30.

order to discard any degradation effects because of applied thermal treatments [20].

The thermal and structural behaviour of these blends in dynamic experiments have been studied before [16]. A depression of the melting transition of N6 has been observed as the liquid crystal content is increased and this behaviour has been related to an improvement of the compatibility between both components in the used crystallization conditions. In contrast, two different polymorphic forms α and γ*, can be observed in N6, depending on the thermal history and humidity conditions. This behaviour is also detected in its blends with Vectra but the liquid crystal component seems to enhance the stability of the α crystalline form.

The crystallization kinetics of the N6 component was analyzed from data obtained in a temperature interval ranging from 200°C to 216°C for all blend compositions. At higher temperatures, the crystallization rate was too slow to be measured by DSC in a reasonable time period, and at lower temperatures, the process was too rapid to preclude accurate measurements. As it was pointed out in a previous paper [16], the enthalpy change associated to the crystallization process of Vectra A is very small and the isothermal ordering can not be detected by the usual calorimetric measurements.

The crystallinity values after the isothermal crystallization were obtained, as it was indicated in the experimental section, using the extrapolated value of the enthalpy corresponding to the melting of the 100% crystalline samples. Crystallinity values around 20% were estimated in all the cases independently of the crystallization temperature.

These data are slightly lower than those determined in the dynamic experiments [16], which can be related to the crystallization of the lower molecular weight species at lower temperatures. However, the crystallinity percentages seem not to be strongly affected by the blend composition in both cases.

The experimental data have been also analysed according to the Avrami equation. The Avrami approximation [21–23] describes the isothermal development of crystallinity in polymers according to the equation:

$$1 - \theta = \exp(-Kt^n) \tag{1}$$

where θ is the fraction of crystallized material at time t, k is a constant and n defines the mode of nucleation and growth. Values of $n = 2$, 3, or 4 have been obtained for the one-, two- and three-dimensional growth geometries, respectively. Several simplifications have been introduced in the Avrami equation, but many polymers show good adherence to this relation, at least for the initial part of the process. Trying to fit the data over the complete crystallization range is an error that can lead to unusual values of the Avrami exponents [1].

From the slope of the plot log [ln(1 − θ)] against log *t* for a conversion range from 5% to 30%, the values of the exponent *n* are obtained as shown in Fig. 1 for the N6 homopolymer and for 90/10 blend composition. The obtained plots are not completely linear and a slight curvature can be observed as the liquid crystal content is increased for the higher crystallization temperatures. Similar plots have been also reported for PET/Vectra blends [3] and this behaviour
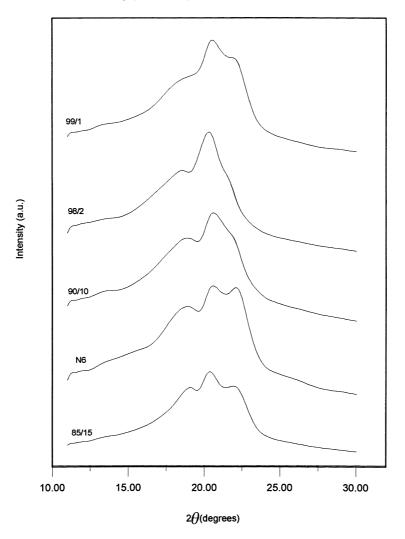
Fig. 4. WAXS diffractograms obtained after isothermal crystallization at 206°C for 15 min for the indicated blend compositions.

has been related to changes in the nucleation mechanism or crystalline geometry.

The mean exponent of the Avrami equation was found to be 4 for the N6 component in all the studied samples, with the exception of the 70/30 composition. In this case, an exponent of $n = 3$ was obtained for the higher temperature range. In previous studies, the isothermal crystallization kinetics of N6/polypropylene blends have been investigated [24,25], and an Avrami exponent of 3 resulted in all cases for the polyamide component, which was independent of the blend composition and the method of preparation. Avrami exponents increasing from 3 to 4 with the crystallization temperature have been reported by several authors [5,8–10,13], and the influence of nucleating agents [9,10], processing methods [12], crystalline structure [7], or superimposition of effects of primary and secondary crystallization [5,10] have also been considered.

Fig. 2 shows the changes in the time to reach the 10% of transformation, $\tau_{0.1}$, as a function of the crystallization temperature for the N6 pure component and in the corresponding blends. In all the cases, $\tau_{0.1}$ increased

exponentially with the temperature, confirming that the ordering process occurred through a nucleation mechanism. As seen in Fig. 2, for the same crystallization temperature, the values of $\tau_{0.1}$ were strongly affected by the liquid crystal content.

This effect is also observed in the corresponding values of constant of crystallization rate as shown in Fig. 3 for different blend compositions. This constant is defined as $K = \ln2/(\tau_{0.5})^n$ where $\tau_{0.5}$ is the time to reach the 50% of transformation and n is the Avrami exponent and gives information about the magnitude of the increase of the crystallization rate [26]. As seen in Fig. 3 K decreases exponentially with the crystallization temperature. The influence of the composition is more important at high undercoolings where the K values are higher than those obtained for N6 and show a dramatic increase for the compostions with higher Vectra content.

In order to clarify this behaviour, WAXS and SAXS experiments were carried out to monitor in real time the isothermal crystallization process by means of synchrotron radiation. It was previously reported [16] that two crystalline forms named as α and γ^* could be observed for the N6
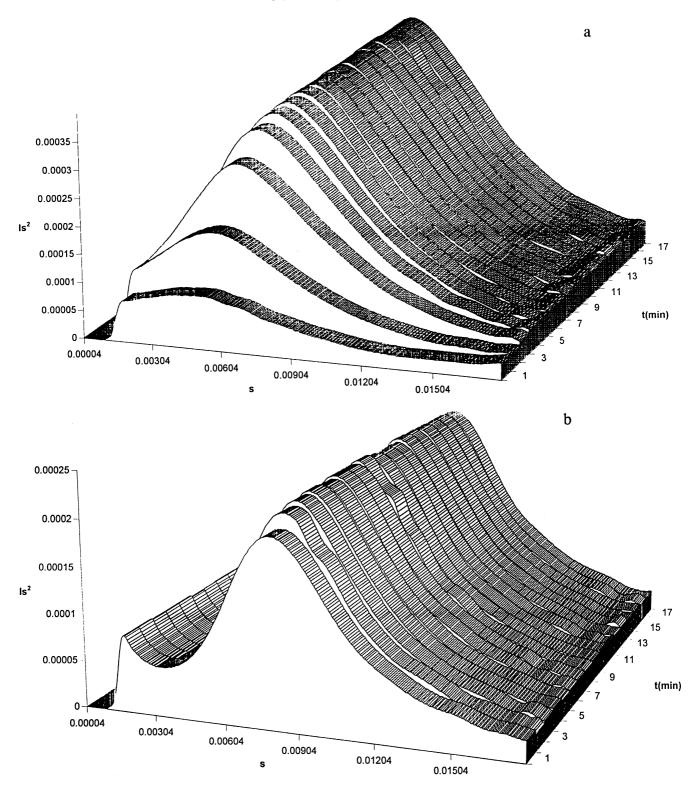
Fig. 5. Plot of scattered intensity as a function of the scattering vector at different crystallization times for the following blend compositions: (a) 100/0 (b) 85/15.

component of these blends. The α form exhibited two reflections at $2\theta = 20°$ and $23°$, whereas only one reflection at $2\theta = 21°$ was observed for the γ^* form. WAXS analysis of original samples at room temperature demonstrated that both polymorphic forms α and γ^* coexist for pure N6, but the reflections associated to the γ^* form almost disappear gradually in the blends as the concentration of liquid crystal polymer increases.
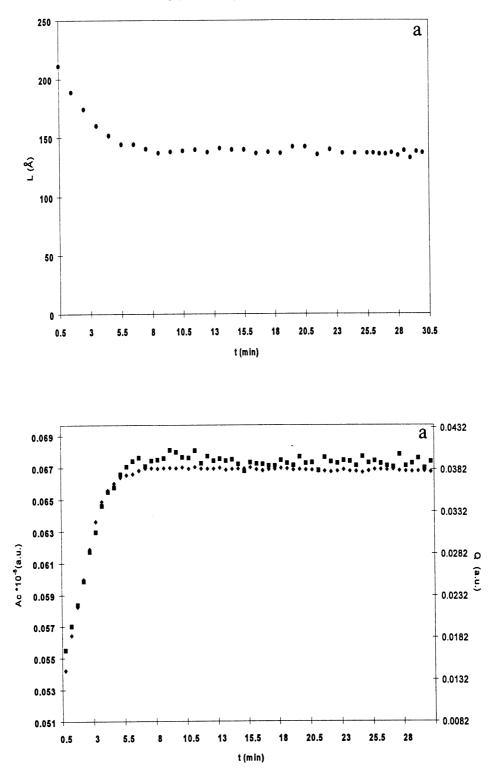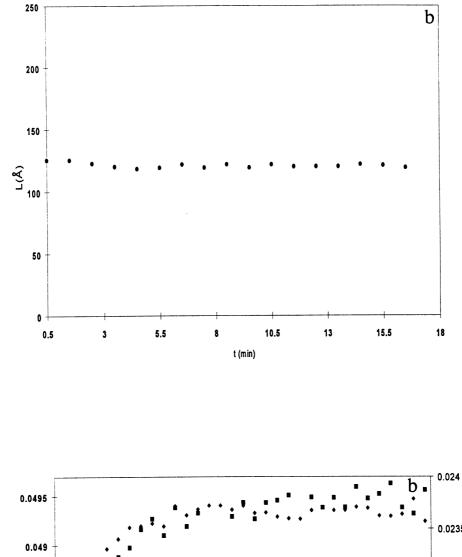
Fig. 6. Plot of the A_c (■), Q (◆) and L (●) values against crystallization time for the following compositions: (a) 99/1 (b)85/15.

The WAXS patterns obtained for different blend compositions isothermally crystallized at 206°C are shown in Fig. 4. These results demonstrated that a mixture of the two crystalline forms was observed when these samples were isothermally crystallized at 206°C after fast cooling from the melt. However, it became clear from the comparison between Figs. 2, 3 and 4 that for the blends with low Vectra content (up to 10%) the γ^* form is predominant after the isothermal crystallization and in these cases, the crystallization rate is lower than that observed for N6 pure homopolymer which shows a mixture of both α and γ^* crystalline forms, but the crystallization rate constants are very similar.
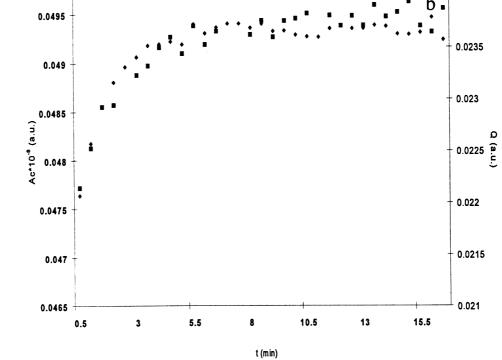
Fig. 6. Continued.

The $\tau_{0.1}$ values at a specific crystallization temperature are lower and the crystallization rate constant are higher as the intensity of the reflections associated to the α form increases for the blends with higher percent of liquid crystal polymer.

It has been previously described that the presence of Vectra favours the formation of the α crystalline form independently of the applied thermal treatment [16] and this behaviour can be related to the changes observed in the crystallization rate. These results also agree with previous data reported in the literature [27] for the melt crystallization of pure N6 homopolymer, showing that the crystallization rate of the α form is higher than that of the γ^* form with increasing crystallization temperature and becomes dominant above 180°C. The liquid crystal component is in solid state at the crystallization temperature range of N6 and can have a nucleation effect on the crystallization process of the polyamide increasing the crystallization rate and favouring the formation of the α form that crystallizes faster in the considered temperature interval. This nucleating activity is observed for the compositions with higher Vectra content as the size of liquid crystal domains becomes larger and coalescence phenomena can occur. However, when the liquid crystal content is 10% or lower, a partial miscibility between the blend components may occur that determine the reduction of the crystallization rate, improving the formation of the γ^* form.

SAXS data were also obtained simultaneously with the WAXS experiments in order to analyse the lamellar morphology. Fig. 5 shows the SAXS scattering patterns obtained for N6 pure component and the 85/15 blend composition isothermally crystallized in the same conditions as indicated above. The scattered intensity (I_s^2) after Lorentz correction was plotted against the scattering vector s ($s = (2/\lambda)\sin\theta$; θ being the scattering angle and λ the wavelength) and the crystallization time. The obtained patterns showed a maximum associated to the polyamide component. The scattering is provoked by the density differences due to the alternation of crystal and amorphous regions and a maximum scattering indicates a good uniformity between the thickness of the crystal, l_c, and the amorphous region, l_a. The long period represents the periodicity of the sum of the crystalline and non-crystalline thickness, which is obtained from the maximum of the SAXS curve as $L = 1/s_{\max}$.

Values of the area under the crystal reflections, A_c, were obtained from the corresponding WAXS patterns and were compared with the corresponding SAXS results. An amorphous halo was subtracted by sketching a base line below the crystal reflections. The shape of this curve approximately corresponds to the diffractogram obtained for the completely molten material. The A_c values are related to the degree of crystallinity (x_c) obtained from WAXS as follows:

$$A_c = \int_0^\infty I_c s^2 \mathrm{d}s, \tag{2}$$

$$x_c = A_c \int_0^\infty I s^2 \mathrm{d}s \tag{3}$$

where I is the total scattering intensity, I_c the scattering intensity of the crystal reflections and s the scattering vector.

Another parameter of interest is the scattering power Q that can be obtained from the SAXS experiments, which can be defined as

$$Q = 4\pi \int_0^\infty I s^2 \mathrm{d}s \tag{4}$$

where I is the scattering intensity normalized to the intensity of primary beam and the volume of the sample. The scattering power can also be defined considering the supramolecular structure:

$$Q = x_S x_L x_{cL}(1 - x_{cL})(\Delta\rho)^2 \tag{5}$$

x_S being the volume fraction filled with spherulites, x_L the volume fraction which has been transformed into lamellar stacks, x_{cL} the crystallinity within the spherulites and $\Delta\rho$ the difference between the densities of the crystallinity and that of the amorphous region. When the growth of the spherulites is over and all the supramolecular structures are completely filled with lamellar stacks, x_S and x_L are equal to 1.

The degree of crystallinity, x_c, can be defined as a function these parameters by the following expresion:

$$x_c = x_S x_L x_{cL} \tag{6}$$

Two different stages can be detected during polymer crystallization as previously reported [28–30]: (a) the primary crystallization is a fast process in which the spherulites grow until they impinge one another. In this case, x_S increases from 0 to 1, but x_L can be considered almost constant; (b) the secondary crystallization is related to additional crystallization within the spherulites. In this case, x_S is equal to 1, but x_{cL} and/or x_L slowly increase. Three different proccesses can occur at this stage: (i) new crystals can grow between the lamellar stacks; (ii) a thickening of the crystals occured while the amorphous regions became thiner; (iii) formation of new lamellar stacks if the spherulites were not fully filled.

The simultaneous study by SAXS and WAXS allows to distinguish between the primary and secondary crystallization, and to determine the mechanisms that contribute to the latter [28–32]. For this purpose, the values of the intensity of the crystal reflections, A_c, the scattering power, Q, and the long spacing, L, were compared (shown in Fig. 6) for different blend compositions.

During the primary crystallization corresponding to the initial stages of the transformation, the values of A_c and Q increased in the same way for all the studied samples, as seen in Fig. 6. According to Eqs. (5) and (6), this behaviour is expected as both parameters follow the same variation with x_S. The sigmoidal forms of the curves can be explained considering the Avrami theory applied to spherulitic growth [21–23,29]. In this theory, the impingement of spherulites is
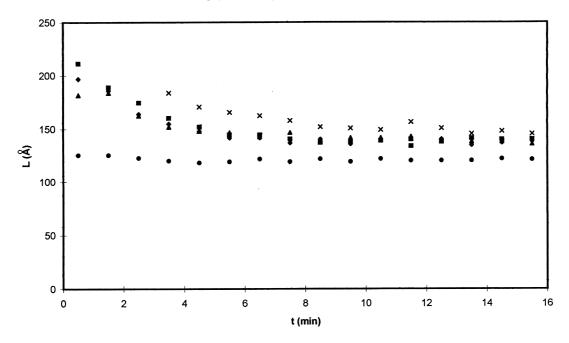
Fig. 7. Plot of the long spacing values versus crystallization time for the following N6/Vectra blend compositions: (◆) 100/0, (■) 99/1 (▲) 98/2 (×) 90/10 and (●) 85/15.

taken account and x_S can be defined as follows:

$$x_S = 1 - \exp(-Kt^n) \qquad (7)$$

where t is the crystallization time, K, a constant depending on the growth rate and n, the Avrami exponent.

The power scattering values, Q, approach to an horizontal asymptote from below without passing through a maximum as shown in Fig. 6. This behaviour permits one to discard the simultaneous concurrency of the secondary crystallization, as it has been previously reported [30]. The maximum observed in the SAXS patterns progressively moved to higher s values and the long spacing values decreased during the primary crystallization process, as shown in Figs. 5 and 6. However, 85/15 blend compositions showed only a slight decrease in the long spacing values with time at this early stage of transformation (Fig. 6). These changes in the long spacing values occured along with an increase of the SAXS integrated intensity in all the cases, as seen in Figs. 5 and 6.

It has been reported by Schultz [30] that the scattering maximum shifts to higher angles and increases in intensity in the crystallization of linear polyethylene. In this case, the primary crystallization process can be interpreted as a model of growing of ''skeletal'' spherulites formed by sequential addition of lamellas to the stack. However, if the maximum grows in intensity, but does not change in position, another model is proposed characterized by the growth of ''dense spherulites'', in which stacks of at least two lamellas grow radially.

In order to explain the decreasing of the long spacing during the primary crystallization process other explanations have been postulated. Bark et al. [28] have considered

the contributions of crystals grown at higher temperature during the cooling process that have longer spacings than those formed during isothermal crystallization. Other authors [29] have pointed out that at the early stages of crystallization, the distances between the crystal lamellas are larger than at the end of the process, and that the formation of new crystal between them during the spherulites growth is possible. The initial decrease of the long spacing has been also interpretated as a consequence of the initial bending of the lamellas [31,32] that decreases during the crystallization process or of the lateral growth and a decrease of the number of defects in the crystalline domains [32].

To clarify this point, the long spacing values obtained for all the blend compositions during the crystallization experiments are plotted as a function of the crystallization time in Fig. 7. A dramatic decrease of the long spacing values with the crystallization time is observed for the lower Vectra content compositions at the early stages of the crystallization process. These results may indicate that a partial miscibility between the blend components occur in the amorphous phase, but the liquid crystal component is progressively excluded from the interlamellar region. In the case of the 85/15 composition, the long period is almost constant with time, and that means that the liquid crystal component is completely rejected from the interlamellar region at the beginning of the process as a consequence of the poor miscibility between the blend components. This behaviour can also be correlated with the effect of blend composition in the crystallization rate and in the crystalline structure described above, as the 85/15 blend composition shows the higher crystallization rate, improving the stability of the α form.
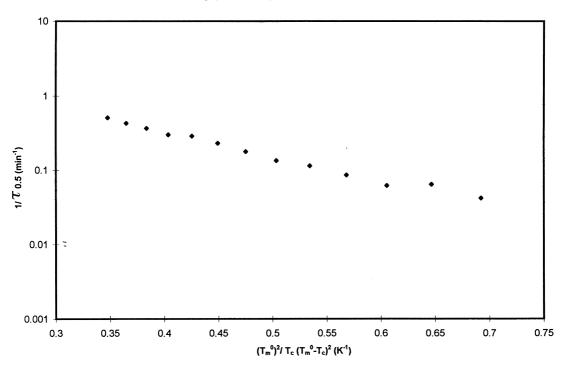
Fig. 8. Plot of log $(\tau_{0.5})^{-1}$ against $(T_m^0)^2/T_c\Delta T^2$ for the 90/10 composition.

During the secondary crystallization, the long spacing values do not change considerably with the crystallization time for all the blends compositions indicating that Vectra A is completly located outside the interlamellar region in all the cases. It is important to remark that the long spacing values measured for these N6/Vectra A blends after isothermal crystallization were in the range of 120–145 Å. These are always higher than those obtained for the crystallized samples under dynamic conditions (80–90 Å) [33]. A limiting value of 165 Å has been reported for a melt crystallized N6 after annealing at 215°C [34]. It is clear from Fig. 7 that the lower long spacing values correspond to the compositions with higher crystallization rate.

An important effect of the blend composition and the crystallization rate could also be observed in the Q and A_c behaviour for the secondary crystallization process. For the lower liquid crystal content blends with lower crystallization rate, the obtained Q and A_c values followed a similar variation pattern with crystallization time. This behaviour indicated that new lamellar stacks were growing and would imply that, according to Eqs. (5) and (6), Q and A_c were proportional to x_L. A similar tendency had been previously observed for the isothermal crystallization of poly (ethylene naphthalene-2,6-dicarboxylate) and a copolymer of poly (vinylidene fluoride) and poly (trifluoroethylene) [29].

For the higher Vectra content compositions, we found that A_c increased with the crystallization time, but Q remained almost constant. This was more evident for those blend compositions in which the crystallization was faster. This behaviour would indicate that, in the secondary crystallization process, the degree of crystallinity within the

lamellar stacks (x_{cL}) increased, while x_L and x_S remained constant. As indicated in Eqs. (5) and (6), A_c is proportional to x_{cL}, but Q is proportional to $x_{cL}(1 - x_{cL})$ and the change of $x_{cL}(1 - x_{cL})$ is very small for typical values of x_{cL} detected in the secondary crystallization. These changes have been also reported for the crystallization of several homopolymers [28,29] and have been related to crystal thickening or formation of new crystals between the existing ones. In the blend compositions studied here, the long spacing values were almost constant for the secondary crystallization, indicating that the crystal became thicker while the amorphous phase between them got thinner.

The kinetic data obtained by calorimetry were also analysed from a thermodynamic point of view. The dependence of the melting temperature after the isothermal crystallization process with the crystallization temperature was analysed, and the equilibrium melting temperature was determined by extrapolating at the line $T_m = T_c$. The corresponding equilibrium melting temperature for the N6 homopolymer is $T_m^\circ = 244°C$, but the values obtained for the N6 component in the blends are slightly lower and do not show any clear dependence on the blend compositions. Different values have been proposed in the literature [5,9–11] for the equilibrium melting temperature of N6 homopolymer ranging from 228°C to 239°C. A depression of the equilibrium melting temperature has been found in other polymer blends [2–4] indicating an improvement of the miscibility between both components. According with the previous discussion about the effect of the composition in the long spacing values during the primary crystallization, the depression of the equilibrium melting temperature observed

for the blends with a Vectra percent up to 10% must be a consequence of the miscibility between both phases in the amorphous region. However, the equilibrium melting temperature obtained for the 85/15 composition is also 6°C lower than that of N6 homopolymer and that must be attributed to the reduction of the crystalline thickness. As it was described above, this crystalline thickness reduction is due to the increase in the crystallization rate as a consequence of the nucleating activity of the liquid crystal component. These data are not in contradiction with a previous study of the thermal properties of the N6/Vectra A blends in dynamic conditions [16] due to the different applied thermal history which can modify the morphology of the different phases. In this case, a depression of the thermal transitions of the polyamide component was related to a better miscibility of the components in blends with higher liquid crystal content.

The values of the equilibrium melting temperature have been used to analyse the temperature coefficient of the process using the following equation:

$$\ln(\tau_{0.5})^{-1} = \ln(\tau_{0.5})_0^{-1} - \frac{K_n}{T_c}\left(\frac{T_m^0}{\Delta T}\right)^n \tag{8}$$

in which $(\tau_{0.5})_0$ and K_n are constants, T_m^0 is the extrapolated melting temperature and ΔT is the undercooling. The exponent n has a value of 2 for three-dimensional homogeneous nucleation and an unity value for coherent two dimensional nucleation. The constant K_n is given by $K_2 = 8\pi\sigma_e\sigma_u^2/R\Delta H_u$ and $K_1 = 4\sigma_e\sigma_u/R\Delta H_u$ for the first and the second case, respectively. ΔH_u is the melting enthalpy for the 100% crystalline polymer and σ_e, σ_u are the product of the lateral and basal interfacial energies.

According to Eq. (8), for $n = 2$, since the Avrami exponent in the crystallization is 4, the value $\sigma_e\sigma_u^2$ has been determined from the plot of $\ln(\tau_{0.5})^{-1}$ against $(T_m^0)^2/T_c\Delta T^2$ (Fig. 8). The obtained values fall in the range 12×10^8–3×10^8 J.mol^{-3} and are in the same order as those obtained for other semi-crystalline polymers [1,35]. The lowest value is obtained for the 99/1 blend composition as this blend shows higher ratio of the γ^* crystalline form. It has been reported [16] that the enthalpy of melting of this crystalline form is much lower than that associated to the α form.

4. Conclusion

The content of the liquid crystal polymer influences the formation of the different polymorphs and therefore, has an strong effect on the isothermal crystallization of N6/Vectra blends. The resulting data has demonstrated that the crystallization rate in these blends is strongly determined by the crystalline structure but no influence was observed on the corresponding Avrami exponents and a value of $n = 4$ was obtained in all cases.

It was shown by WAXS experiments using synchrotron radiation that the crystallization process is slower when the γ^* crystalline form is observed. The more stable the α form is during the crystallization process, the higher is the crystallization rate. The SAXS data demonstrated that the changes in the crystalline structure and in the crystallization rate can be correlated with different mechanisms observed for the primary and secondary crystallization processes.

The equilibrium melting temperatures after isothermal crystallization were determined by an extrapolated method and a depression of these values observed in the blends has been attributed to a better compatibility between the components in the amorphous phase for the low Vectra content compositions.

Finally, the temperature coefficients of the transformation were also determined and the obtained values for the product of the interfacial free energies showed values comparable with those found for other semi-crystalline polymers.

References

[1] Fatou JG. Encyclopedia of polymer science and engineering. Suppl. 231: New York: Wiley, 1989.
[2] Martuscelli E. Polym Eng Sci 1984;24:563.
[3] Chang-Chien GP, Denn MM. Polym for Adv Tech 1995;7:168.
[4] Carvalho B, Bretas RES. J Appl Polym Sci. 1995;55:233.
[5] Tomka T, Sebenda J, Wichterle O. J Polym Sci Part C 1967;16:53.
[6] Brucato V, Piccarolo S, Titomanlio G. Makromol Chem Macromol Symp 1993;68:245.
[7] Bruccato V, Crippa G, Piccarolo S, Titomanlio G. Polym Eng Sci 1991;31:1411.
[8] Hinrichsen G, Lux F. Polym Bull 1990;24:79.
[9] Eder E, Wlochowicz A. J Therm Analys 1989;35:751.
[10] Wlochowicz A, Eder M. Coll Polym Sci 1983;261:621.
[11] Burnett B, McDevit WF. J Appl Phys 1957;28:1001.
[12] Khanna YP, Reimschussel AC, Banerjie A, Altman C. Polym Eng Sci 1988;28:1600.
[13] Turska E, Gogolewski S. Polymer 1971;12:616.
[14] Starkweather HW, Brooks RE. J Appl Polym Sci 1959;1:236.
[15] Müller A, Pflüger R. Kunststoffe 1960;50:203.
[16] Campoy I, Gómez MA, Marco C. Polymer 1998;39:6279.
[17] Fatou JG, Barrales J M. J Polym Sci Part A-2 1969;7:1755.
[18] Inoue M. J Polym Sci Part A 1963;1:2697.
[19] Elsmer G, Rickel C, Zachmann HG. Adv Polym Sci 1985;67:1.
[20] Campoy I, Gómez MA, Marco C. J Therm Analys 1998;52:705.
[21] Avrami M. J Chem Phys 1939;7:1103.
[22] Avrami M. J Chem Phys 1940;8:212.
[23] Avrami M. J Chem Phys 1941;9:177.

[24] Campoy I, Arribas JM, Zaporta MAM, Marco C, Gómez MA, Fatou JG. Eur Polym J 1995;31:475.

[25] Marco C, Ellis G, Gómez MA, Fatou JG, Arribas JM, Campoy I, Fotecha A. J Appl Polym Sci. 1997;65:2665.

[26] Kim SP, Kim SC. Polym Eng Sci 1991;31:110.

[27] Kyotani M, Mitsuhashi S. J Polym Sci Part A-2 1972;10:1497.

[28] Bark M, Zachmann HG, Alamo R, Mandelkern L. Makromol Chem 1992;193:2363.

[29] Zachman HG, Wutz C. Crystallization of polymers. In: Dosiere M, editor. Dordrecht: Kluwer Academic Publisher, 1993:403.

[30] Schultz JM. Makromol Chem Macromol Symp 1988;15:339.

[31] Elsner G, Zachmann HG, Milch JR. Makromol Chem 1981;182: 657.

[32] Elsner G, Koch MHJ, Bordas J, Zachmann HG. Makromol Chem 1981;182:1263.

[33] Campoy I, Gómez MA, Marco C. Manuscript in preparation.

[34] Gogolewski S, Gasiorek M, Czerniawska K, Pennings AJ. Polym Sci 1982;260:859.

[35] Wunderlich B. Macromolecules physics, vols. 1–3 New York: Academic Press, 1973, 1976, 1980.